**Supporting Information**

# Immobilization of Dye Pollutant on Iron Hydroxide Coated Substrates: Kinetics, Efficiency and Adsorption Mechanism

Junyi Liu,[ab] Lai Mun Wong,[b] Gurudayal,[c] Lydia Helena Wong,[c] Sing Yang Chiam,[*b] Sam Fong Yau Li[*a] and Yi Ren[*b]

[a]*Department of Chemistry, National University of Singapore, 3 Science Drive 3, 117543 Singapore. Email: chmlifys@nus.edu.sg*

[b]*Institute of Materials Research and Engineering, Agency for Science, Technology and Research, 2 Fusionopolis Way, 138634 Singapore. Email: chiamsy@imre.a-star.edu.sg, reny@imre.a-star.edu.sg*

[c]*Solar Fuels Lab, School of Materials Science and Engineering, Nanyang Technological University, 50 Nanyang Avenue, 639798 Singapore*

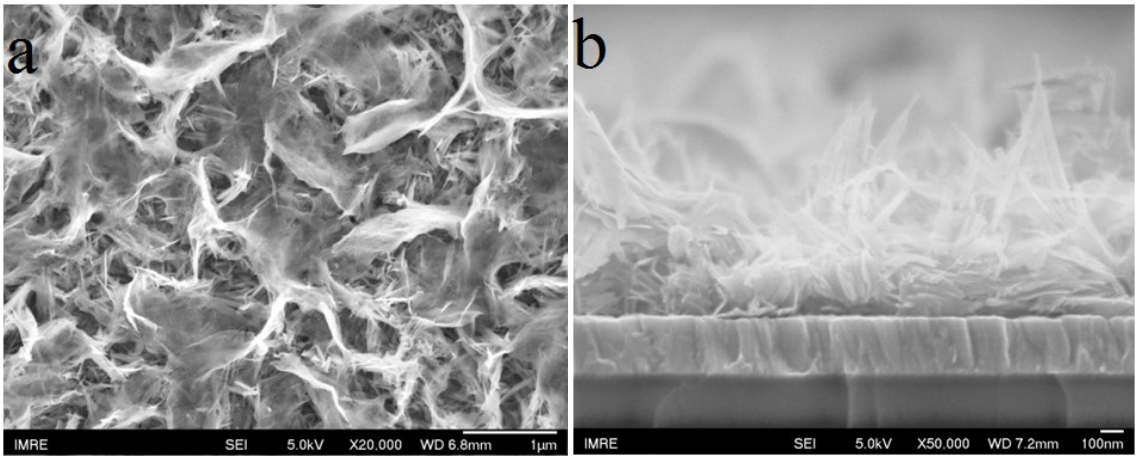


Figure S1 SEM images of (a) surface and (b) cross-section of the FeOOH films deposited with 0.5 M $(NH_4)_2Fe(SO_4)_2$ and 1 M $CH_3COONa$ under a high growth rate. Large and flaky structures with poor adhesion and uniformity are observed.

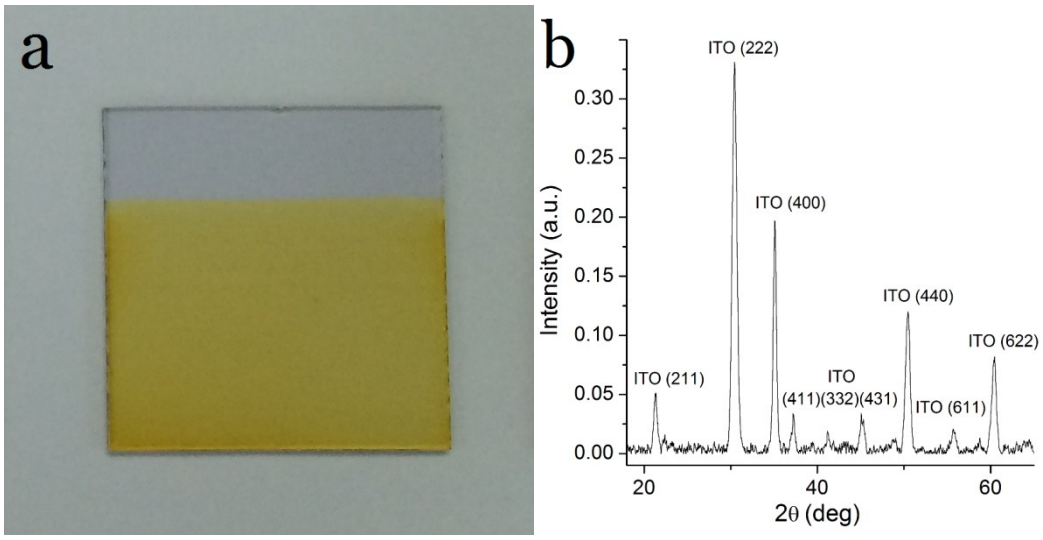


Figure S2 (a) Picture of FeOOH film deposited on ITO under optimized condition showing good uniformity. (b) X-ray diffraction spectrum of the coated FeOOH on ITO. Only diffraction peaks of ITO were observed showing the amorphous nature of the film.

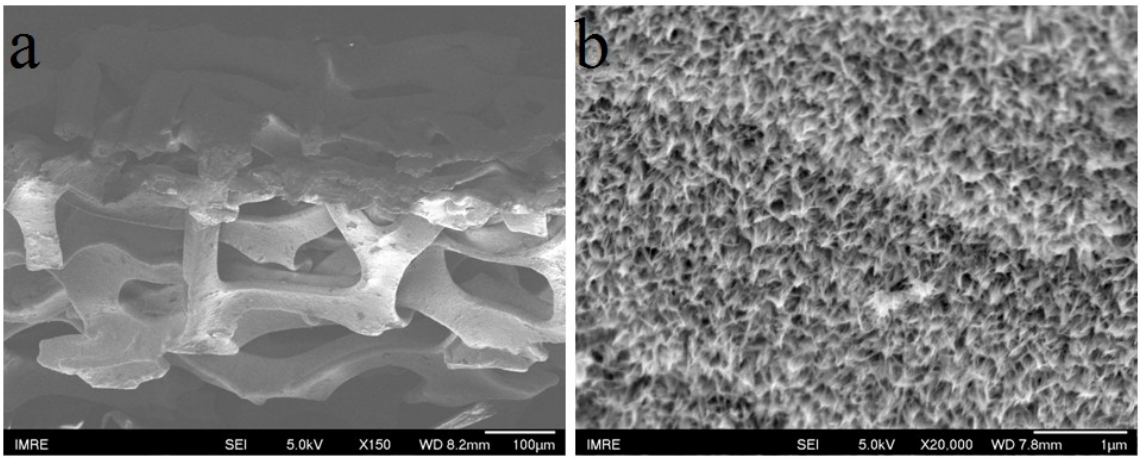


Figure S3 SEM images of the electrodeposited FeOOH films on Ni foam substrate with (a) low and (b) high magnification. The images show the growth of porous structures on the surface of the Ni foam.

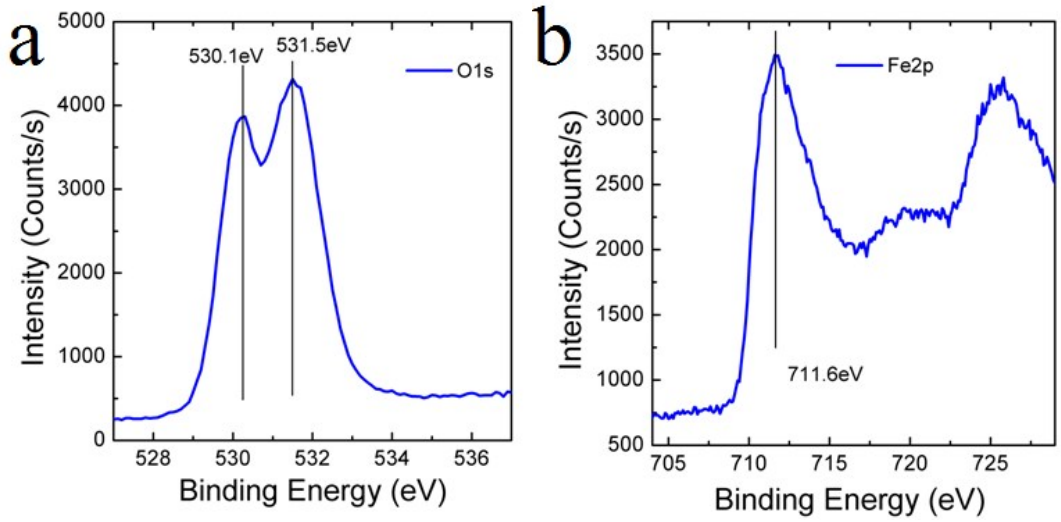


Figure S4 X-ray photoelectron spectra of (a) O 1s and (b) Fe 2p of the FeOOH film deposited on ITO. The binding energy for both O 1s and Fe 2p is consistent with the presence of FeOOH.

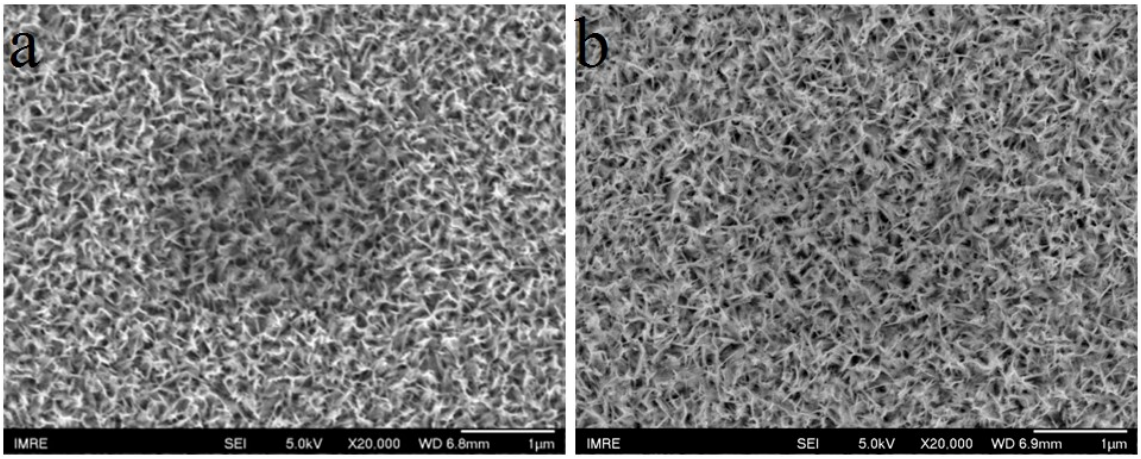


Figure S5 SEM images of FeOOH film (a) before and (b) after the adsorption of Congo red. The images show similar morphology indicating the absence of major structural change.

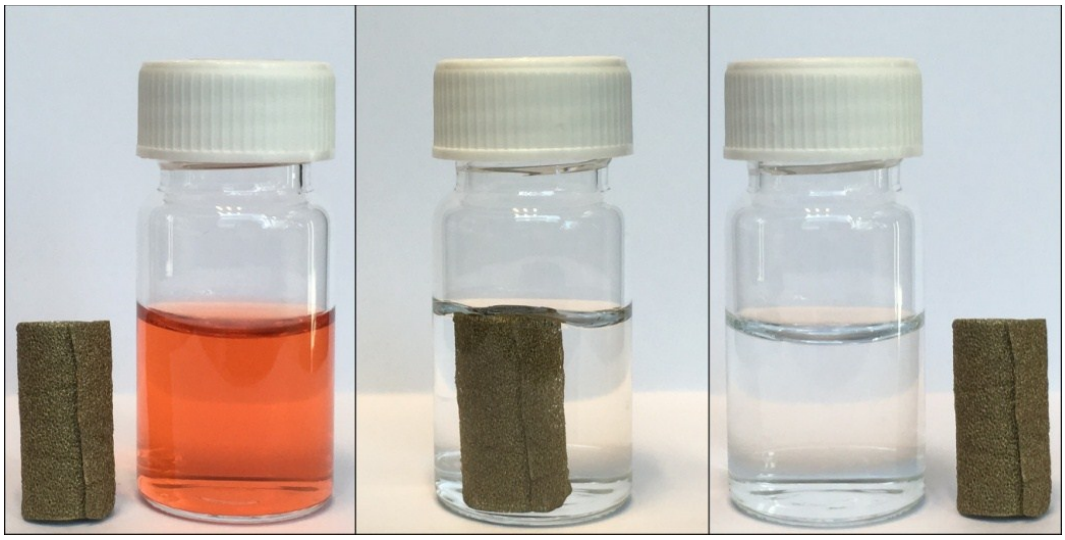

Figure S6 Images of 10 mL of 20 mg/L Congo red solution (left), the solution after 180 minutes immersion of coated FeOOH on Ni foam (middle) and the solution after removal of coated film and contaminants (right). The process above demonstrated easy immobilization and removal of dye pollutant.

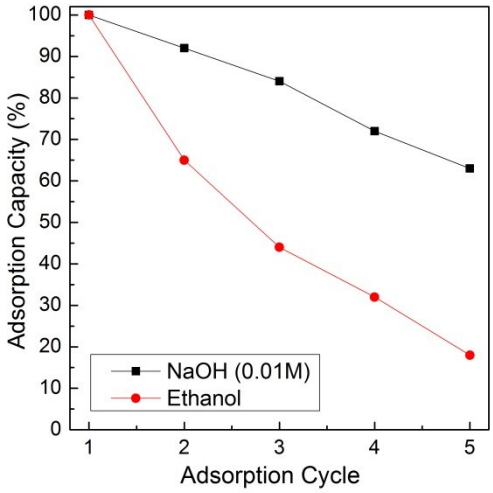


Figure S7 Relative adsorption capacity of the coated FeOOH with respect to the initial adsorption for 5 cycles of adsorption and desorption process. The desorption process was accomplished by a 1 hour soaking in the indicated solutions. We found that each cycle of

adsorption achieved on average 88.9% and 65.1% of the previous adsorption capacity in NaOH solution and ethanol, respectively.

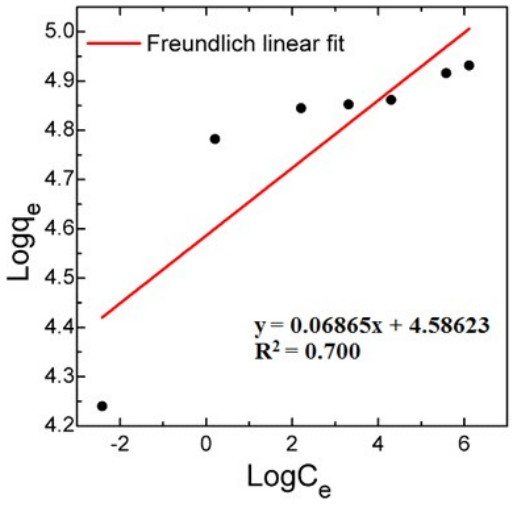


Figure S8 Linearized Freundlich isothermal plots of Congo red adsorption on FeOOH film. A poor correlation coefficient of 0.7 is obtained showing a lack of multilayer adsorption.

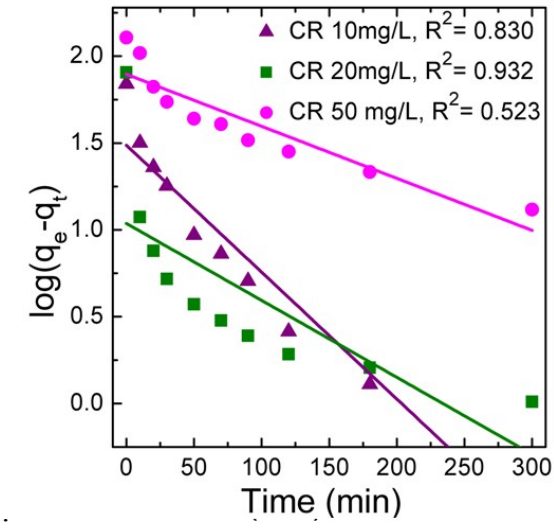


Figure S9 Linearized pseudo-first-order kinetics plots of Congo red adsorption for FeOOH deposited on Ni foam. Poor correlations are obtained for all different Congo red concentrations. The correlation coefficient for each concentration is indicated in the plot.

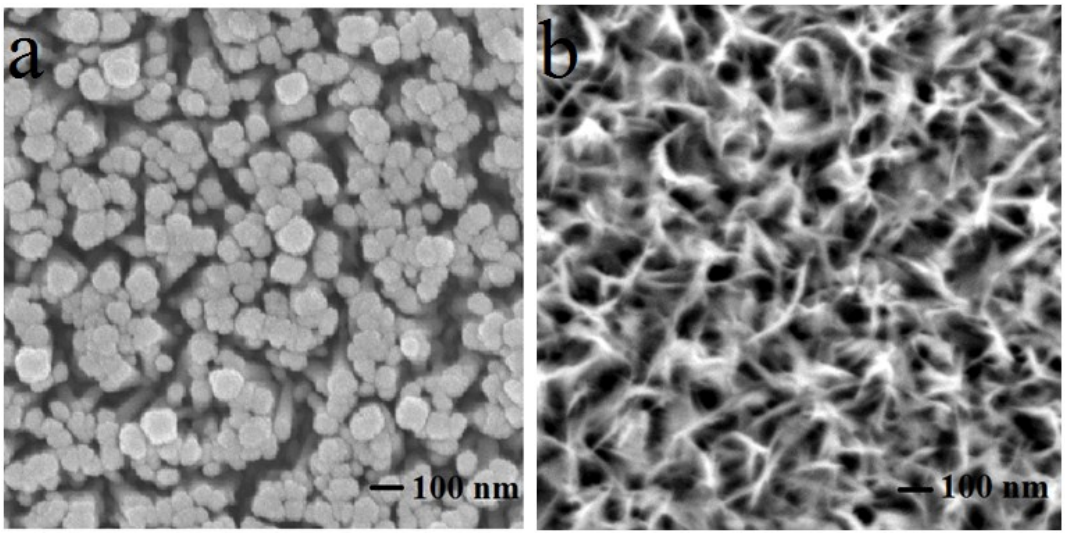


Figure S10 SEM images of (a) hydrothermally grown FeOOH and (b) electrodeposited FeOOH. The hydrothermally grown sample was accomplished by 6 hours of reaction at 100 °C in 10 mL of aqueous solution containing 1.5 mmol $FeCl_3$•$6H_2O$ and 1.5 mmol $NH_2CONH_2$. The measured capacity of ~40 mg/g for hydrothermal grown FeOOH is lower than electrodeposited FeOOH reported in this work.

Table S1 A comparison of Congo red adsorption properties of various iron oxide/hydroxide nanostructures

| **Adsorbents** | **$q_m$ (mg/g)** | **References** | **Year** |
|---|---|---|---|
| **Coated porous FeOOH thin film** | 144 | This work | 2015 |
| **Coated FeOOH rods** | 41 | This work | 2015 |
| **Conventional FeOOH** | 32 | 18 | 2013 |
| **Commercial α-$Fe_2O_3$** | 42 | 35 | 2014 |
| **α-FeOOH hierarchical nanostructure by self-assembly** | 56 | 18 | 2013 |

| | | | |
|---|---|---|---|
| **Urchin-like α-FeOOH hollow spheres** | 275 | 16 | 2012 |
| **α-FeOOH hierarchical nanostructure** | 239 | 17 | 2011 |
| **Mesoporous Fe2O3** | 53 | 34 | 2008 |
| **γ-Fe2O3 hierarchical nanostructure** | 58 | 18 | 2013 |
| **α-$Fe_2O_3$ hierarchical nanostructure** | 66 | 17 | 2011 |
| **Hollow nestlike α-$Fe_2O_3$** | 160 | 29 | 2012 |
| **α-$Fe_2O_3$ nanoparticles** | 254 | 35 | 2014 |
| **α-$Fe_2O_3$ hollow spheres** | 195 | 31 | 2013 |

Table S2 Kinetic parameters and correlation coefficients calculated from pseudo-second-order model for adsorption of Congo red on FeOOH film

| **Congo red concentration (mg $L^{-1}$)** | **$q_{e,exp}$ (mg $g^{-1}$)** | **$q_{e,cal}$ (mg $g^{-1}$)** | **$k_2$ (g $mg^{-1}$ $min^{-1}$)** | **$R^2$** |
|---|---|---|---|---|
| 10 | 70.351 | 71.582 | $1.789\times 10^{-3}$ | 0.999 |
| 20 | 82.637 | 84.034 | $6.316\times 10^{-4}$ | 0.999 |
| 50 | 128.079 | 123.001 | $3.332\times 10^{-4}$ | 0.998 |